

Hardness and tribological properties of laser irradiated PMMA based nano-microcomposites

Hebatalrahman A. HEBATALRAHMAN 

Independent Researcher, Cairo, Egypt
hebatalrahman11@gmail.com

Keywords

structure
hardness
wear
PMMA
random distribution

History

Received: 27-02-2022
Revised: 19-03-2022
Accepted: 27-03-2022

Abstract

In this work, new composite material is manufactured from poly(methyl methacrylate) PMMA matrix reinforced by glass fibre type E-glass. The effect of volume fraction of fibre and length to diameter ratio is studied, and friction and wear characteristics were determined at different volume fractions and fibre sizes. The hardness and wear resistance of randomly distributed PMMA matrix composite were significantly enhanced, and the maximum conditions for reinforcement of PMMA matrix composite to improve tribology characteristics were evaluated. The effect of laser irradiation on the mechanical properties was evaluated by irradiation of composite material after manufacturing, with different kinds of lasers. The continuous wave (CW) argon-ion laser and pulsed Nd:YAG laser were used to irradiate composite material. Hardness, wear rate, and coefficient of friction were evaluated at the same test condition of the unirradiated composite. The significant improvement in improvement in the mechanical properties at certain irradiation conditions was evaluated.

1. Introduction

Composite will not, split, delaminate or absorb moisture. Therefore, its life span will be many times more than traditional materials. Fibres are the commonly used reinforcement in many types of composites. If the fibre density is known we also have a fibre diameter, otherwise it is simpler to measure diameters in micro [1]. Microfibers in technical fibres refer to ultrafine fibres (glass or melt blown thermoplastics) often used in filtration. Newer fibre designs include extruding fibre that splits into multiple finer fibres [2-5]. Polymer-based composites with randomly distributed filler are used in a wide range of applications in aerospace, marine, automotive, surface transport and sports equipment markets. Damage to composite components is not always visible to the naked eye and the extent of damage is best determined for structural components [6].

Polymers are used in tribological applications for many reasons. In many instances, polymers perform a dual function as both a structural and a tribological material. An example of dual functionality is self-lubricated polymers. Concerns such as weight, cost, and ability of manufacturing are some of the same issues with the use of polymers and polymeric composites for sliding applications as in structural applications. Polymer failure in tribological applications is often catastrophic and occurs in a very short time scale. The work was performed with curved short glass fibres and has found great applicability in the contact and subsequent friction of electrometric sliding. However, the glass is rough and the real contact is reduced from the Hertzian contact area [7]. In this work, the effect of laser irradiation on the tribology was detected as a new technique in composite material worlds.

2. Experimental work

2.1 Materials

Matrix: The matrix is poly(methyl methacrylate) (PMMA). It is thermoplastic prepared from

monomer (methyl methacrylate) by an additional polymerization process; polymer was in the granule form [8-10].

Filler: Glass fibre (brand milled fibres) are glass filaments coated with a specific sizing to enhance resin compatibility and hammer milled to a specified bulk density. Fibres are hammered and milled to an average fibre length. Average fibre length is determined by the input glass and process conditions. In the current work, milled fibres are made from E-glass (electrical) which conforms to MIL-R-60346C specification with an average bulk density of 0.55 g/cm^3 in floccular and powder form with length to diameter ratio ($L/D = 50$ and, $L/D = 1$) respectively [11].

2.2 Preparation of material

Grinding: A blinder with variable speeds is used to change the pieces of thermoplastics into powder form. The blinder speed is about 15,500 rpm, works at 200 V and 50 Hz, and the grinding time is about 90 s. Switch off for cooling is lasted about 180 s to prevent the agglomeration of the particles and achieve a reasonable degree of quality in grinding. The retained granules after sieving will be returned to the blinder [12].

Mixing: Automatic mixing for thermoplastic in the powder form with short fibres at different aspects ratio was done. The amount of material required was calculated by changing the volume fraction percent into weight percent ($L/D = 50$ and $L/D = 1$), respectively [13]. The material is prepared by grinding and mixing of thermoplastic in powder form. The process is done with certain volume fractions depending on the properties required in the final composite. The composite material finds finally in the solid form and has different characteristics depending on the fibre percentages (volume fraction of fibres from 17 to 65 %) and fibre size (length to diameter ratio = 50 and 1).

Manufacturing process: Plastic powders and short fibres were mixed together in the solid state. The mixture is heated at the required temperature from 300 to 400 °C, according to its components. The heating rate depends on the type of the joining material; compression and cooling were done for the heated mixture. The new composite material is distinguished with its lightweight and the ability to endure scratch and with damping capacity. It is also liable for the easy formation and is distinctive with different colours and shapes. Figure 1 shows the composite material manufacturing machine.



Figure 1. Composite material manufacturing machine [14]

2.3 Laser irradiation

Samples used in this investigation were in the shape of disks of 25 mm in diameter and 7 mm length (pin dimension used in current work). The irradiation is done on both sides of the samples in different positions to cover all the areas of the sample and achieve a homogeneous surface suitable for testing. The different laser irradiated samples under different conditions were examined before and after laser irradiation and the effect of the laser was determined.

CW argon-ion laser irradiation: The model of the laser device used in current work is Innova-400, which has a power of 25 W and multi-line wavelength from 514.5 to 465.5 nm. The power used in the experiment is 1 W.

Pulsed Nd-YAG laser irradiation: The first harmonic lies in the IR region (wavelength = 1064 nm) with the power of about 60 mW, duration time 6 ns, repetition rate 10 Hz and energy of 360 mJ/pulse. The third harmonic generation (wavelength = 355 nm) in the UV range, power 10 mW, duration time 7 ns, repetition rate 17 Hz and energy of 40 mJ/pulse.

2.4 Mechanical tests

Hardness: The hardness of the specimens was measured by using means of Barcol impressor

according to ASTM D2583 and indenter cone with 26° and 0.157 mm in diameter. The sample must have a smooth and polished surface with specified thickness; the load ranges from 6.8 to 4.5 kg; each hardness value is an average of 29 reading for every specimen. Five specimens at each condition were examined. The measurements are good up to $\pm 6\%$.

Friction and wear testing: The test was carried out in a normal atmosphere including weighing the test specimen before and after the test for assessing the wear properties in such contacts. Pin-on-disc wear test machine (tribometer) is used in this work. The tested specimen was held in sliding contact with rotating hardened alloy steel (Mn-Cr) disc with hardness (HRC 65). The test specimen is mounted to the holder which was designed for easy change of pin (tested samples). The normal load of about 0.06 N/mm^2 is applied by dead weight at the end of the level to cause the actual normal applied load on the test specimen to increase by a factor (lever ratio = 2.75). At the end of the loading beam, there was a counterweight for opposing the beam weight, so the applied forces on the specimen come from the applied dead weight only causing a sliding speed of about 0.13 m/s applied for 10 min. The friction force between the vertical stationary specimen and rotation hardened steel disc was measured by strain gauges fixed on a cantilever attached to the tribometer. From the signal, strain gauges were fed through an electric circuit model F10MK11 which is the standard circuit for strain gauge. Digital strain bridge reading is calibrated to read frictional force value by applying known dead weight later on the arm. The effect of Barcol hardness number of different specimens on properties is recorded. Friction and wear value is an average of 3 reading for every condition specimen. The measurements are good up to $\pm 10\%$.

The coefficient of friction is determined by:

$$U = \frac{F}{W} \quad (1)$$

where U is the coefficient of friction, F is the friction force and W is the normal load.

The wear volume is calculated from the relation:

$$V = \frac{w}{\rho} \quad (2)$$

where V is wear volume, w is the wear weight (the difference in weight of specimen before and after the test) and ρ is the density of composite.

Table 1 shows the density of the composite material at a different volume fraction of fibres and different length to diameter ratios.

Table 1. The density of the composite material at a different volume fraction of fibres and different length to diameter ratio

Specimen No.	L/D	Fibre volume, %	Density, gm/cm^3
1	0	0	1.120
2	1	17	1.191
3	1	35	1.224
4	1	50	1.246
5	1	65	1.247
6	50	17	1.342
7	50	35	1.327
8	50	50	1.584
9	50	65	1.729

The sliding distance calculated from the relation:

$$L = 2\pi r N, \quad (3)$$

where L is sliding distance (determined to be 78.5 m), r is the mean radius of the rotating disc and N is the number of revolutions.

The following relation is used to calculate the wear coefficient:

$$V = k \frac{LW}{3P}, \quad (4)$$

where V is the wear volume, k is the wear coefficient, L is the sliding distance, W is the normal load and P is the indentation hardness of the softer body.

3. Results and discussion

3.1 Hardness

Barcol hardness of composite is evaluated at different volume fractions of fibre, i.e. at 5 (extra point), 17, 35, 50, and 65 %, at different lengths to diameter ratios. The hardness value is a strong function of the amount of reinforcement presented, due to the manufacturing process. The maximum value was recorded for laser irradiated structures at 50 % volume fraction fibres when the fibre size (length to diameter ratio) $L/D = 50$ and the minimum one was recorded for unreinforced plastics at fibre size $L/D = 1$. Standard deviation is $\pm 6\%$.

The correlation between the Barcol hardness of the composite specimen and the amount of total

fibres volume fraction at different laser irradiation conditions is shown in Figure 2. Figure 3 shows the same correlation at different fibre sizes (length to diameter ratio) $L/D = 50$. It is clear that hardness increases by increasing the amount of fibre which may be attributed to the accumulative strain hardening effect. The laser irradiation conditions, including the type of laser used and the amount of energy absorbed, have a significant effect on hardness. The CW laser at 510 nm in the visible range has the ability to improve the mechanical characteristics of the composite material relative to ultraviolet light at 355 nm.

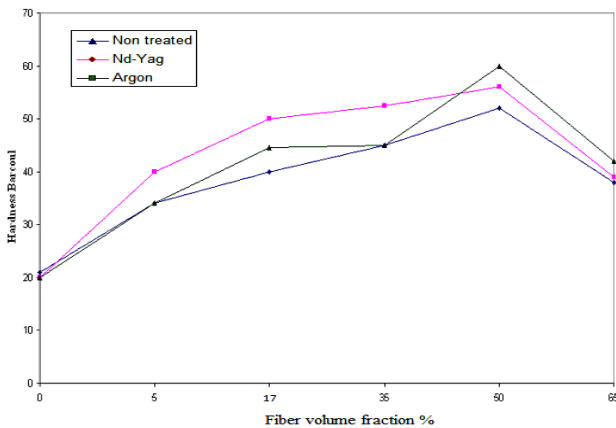


Figure 2. The effect of fibre volume fraction on hardness at $L/D = 1$; adapted from Ahmed [15], licensed under CC BY 3.0

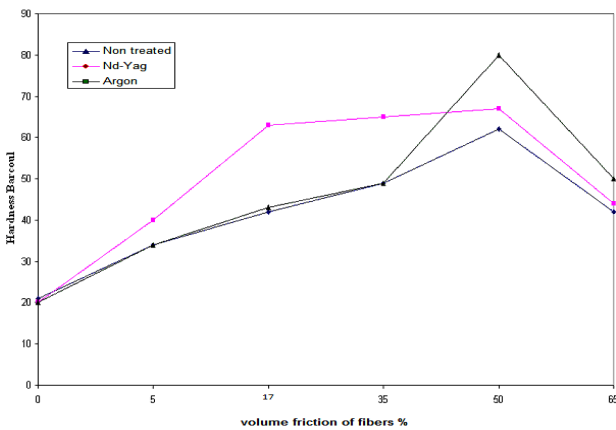


Figure 3. The effect of fibre volume fraction on hardness at $L/D = 50$; adapted from Ahmed [15], licensed under CC BY 3.0

3.2 Friction

The friction behaviour of different conditions was a function of hardness. Figures 4 and 5 show the effect of fibre volume percentage on the coefficient of friction under different conditions, for unirradiated and irradiated composite materials at fibre sizes $L/D = 1$ and $L/d = 50$, respectively. Dry friction arises from a combination

of inter-surface adhesion, surface roughness, surface deformation and surface contamination. The friction force is always exerted in a direction that opposes movement (for kinetic friction). The origin of kinetic friction at the nanoscale can be explained by thermodynamics [16]. Upon sliding, new surface forms at the back of sliding true contact, and the existing surface disappears at the front of it. Since all surfaces involve the thermodynamic surface energy.

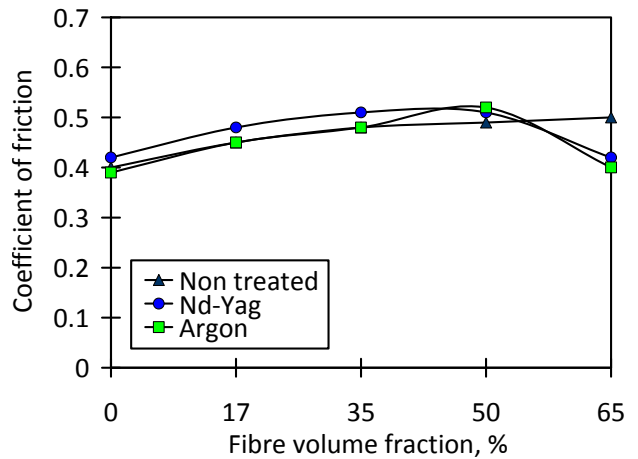


Figure 4. The effect of fibre volume fraction on the coefficient of friction at $L/D = 1$

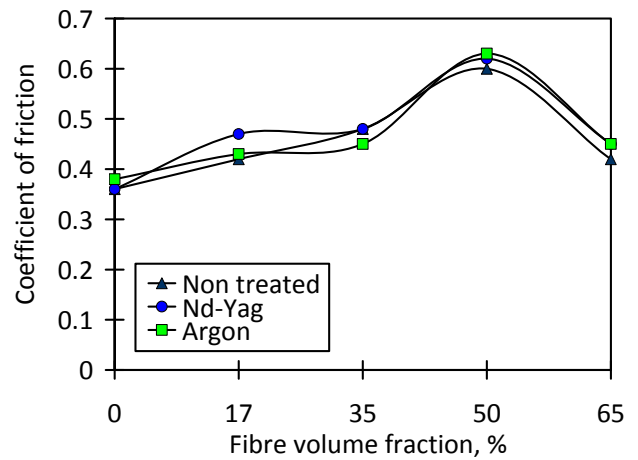


Figure 5. The effect of fibre volume fraction on the coefficient of friction at $L/D = 50$

3.3 Wear

Increasing the length to diameter ratio L/D from 1 to 50 leads to an increase in the resistance of surfaces to penetration, so the hardness value increased at the same volume fraction of fibres. The increase in fibre volume fraction from 17 to 50% increase also surface resistance which leads to a decrease in wear rate. The wear-tested specimens at constant load and constant sliding speed are dependent on the hardness and microstructures of tested specimens. During the

wear test sliding deformation of the surface may occur. Figures 6 and 7 show the wear rate as a function of the fibre volume fraction for unirradiated and irradiated composite materials at fibre sizes $L/D = 1$ and $L/D = 50$, respectively.

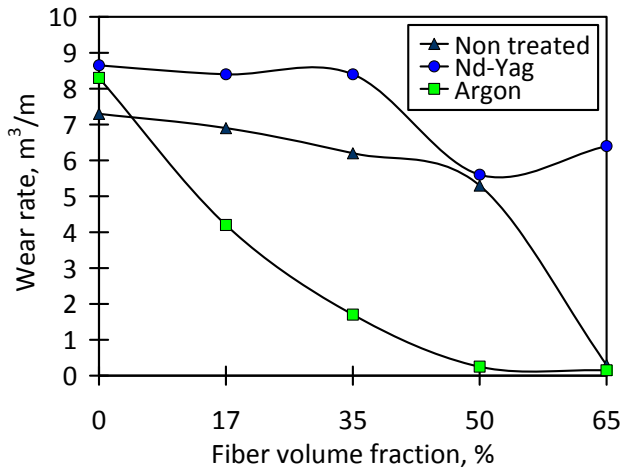


Figure 6. The effect of fibre volume fraction on wear rate at $L/D = 1$

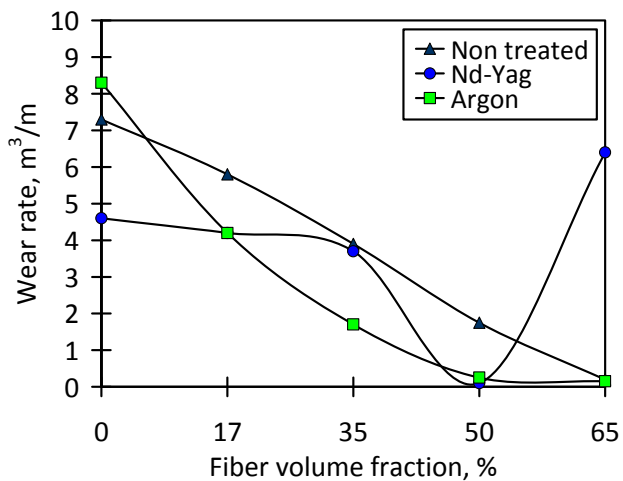


Figure 7. The effect of fibre volume fraction on wear rate at $L/D = 50$

The wear resistance is also influenced by the particles from the cylindrical shape (length to diameter ratio, $L/D = 50$) that has superior wear resistance. During the initial sliding of composite reinforced by fibres, the basal planes of composite shear appear and provide a continuous source of a solid lubricant due to the crystallographic structure. Particles are detached from the composite and the result will be the generation of series of micro-voids and there is act as self-lubrication. Various types of damage have been observed on the sliding surface, such as removal of particles from the matrix of test specimens, reduced deformation, micro-cutting and tearing in-depth, so the loose of particles is the source of self-lubrication.

Work must be spent on creating the new surface, and energy is released as heat in removing the surface. Thus, a force is required to move the back of the contact, and frictional heat is released at the front. However, it does affect kinetic friction for micro- and nano-scale objects where surface area forces dominate inertial forces, to be primarily caused by chemical bonding between the surfaces, rather than interlocking [17].

The improvement in the resistance to surface penetration leads to improve in hardness and wear resistance increases with fibre volume fraction to a certain limit, it reaches the maximum value at 50 % fibre percentages, when increasing fibre volume fraction up to 65 %, both hardness and wear rate decreased to the lower level. The matrix will not be able to bind the additives at higher concentrations. Each fibre concentration depends on the type of laser used which leads to a change in the amount of energy absorbed. The amount of laser energy absorbed is the function of fibre size. The spherical particles (length to diameter ratio, $L/D = 1$) have a smaller surface area for the same volume compared with cylindrical ones (length to diameter ratio, $L/D = 50$).

During laser irradiation, when the amount of laser energy goes through the semi-transparent material, the laser will not be coherent inside the composite specimen, the laser is scattered when striking the particles inside the structure, and the scattering rate depends on the amount of fibre particles inside the structure, especially its shape and distribution.

4. Conclusions

Laser irradiation can improve properties such as hardness and wear.

Hardness increases linearly with an increase in the percentage of fibre. The fibre percentages have a significant effect on hardness and wear.

Friction coefficient decrease with increasing of fibre percent which may be attributed to stress concentration in the vicinity of nodules that work as the self-lubricant element.

Superior wear properties were related to size and amount of reinforcement because fibre work as a self lubricant, minimizing wear.

References

- [1] G. Dyakov, S.V. Burov, P.N. Belkin, E.V. Rozanov, S.A. Zhukov, Increasing wear and corrosion

- resistance of tool steel by anodic plasma electrolytic nitriding, *Surface and Coatings Technology*, Vol. 362, 2019, pp. 124-131, DOI: [10.1016/j.surfcoat.2019.01.107](https://doi.org/10.1016/j.surfcoat.2019.01.107)
- [2] B.S. Mitchell, *An Introduction to Materials Engineering and Science: For Chemical and Materials Engineers*, John Wiley & Sons, Hoboken, 2004.
- [3] L.S. Kumosa, M.S. Kumosa, D.L. Armentrout, Resistance to brittle fracture of glass reinforced polymer composites used in composite (nonceramic) insulators, *IEEE Transactions on Power Delivery*, Vol. 20, No. 4, 2005, pp. 2657-2666, DOI: [10.1109/TPWRD.2005.852289](https://doi.org/10.1109/TPWRD.2005.852289)
- [4] J.M.F. de Paiva, S. Mayer, M.C. Rezende, Comparison of tensile strength of different carbon fabric reinforced epoxy composites, *Materials Research*, Vol. 9, No. 1, 2006, pp. 83-89, DOI: [10.1590/S1516-14392006000100016](https://doi.org/10.1590/S1516-14392006000100016)
- [5] D.R. Askeland, P.P. Phulé, *The Science and Engineering of Materials*, Thomson Brooks/Cole, Pacific Grove, 2003.
- [6] Y. Wang, G. Song, W. Niu, Y. Chen, Optimized design of spray parameters of oil jet lubricated spur gears, *Tribology International*, Vol. 120, 2018, pp. 149-158, DOI: [10.1016/j.triboint.2017.12.042](https://doi.org/10.1016/j.triboint.2017.12.042)
- [7] W.D. Callister, Jr., *Materials Science and Engineering: An Introduction*, John Wiley & Sons, New York, 2003.
- [8] S. Basseville, M. Niass, D. Missoum-Benziane, J. Leroux, G. Cailletaud, Effect of fretting wear on crack initiation for cylinder-plate and punch-plane tests, *Wear*, Vol. 420-421, 2019, pp. 133-148, DOI: [10.1016/j.wear.2018.12.059](https://doi.org/10.1016/j.wear.2018.12.059)
- [9] R.A. Higgins, *Materials for Engineers and Technicians*, Newnes, Oxford, 2006.
- [10] H. Kaiser, V.M. Karbhari, *Quality and Monitoring of Structural Rehabilitation Measures. Part 1: Description of Potential Defects*, University of California, San Diego, 2001.
- [11] İ. Hacısalihoğlu, F. Yıldız, A. Çelik, Tribocorrosion behavior of plasma nitrided Hardox steels in NaCl solution, *Tribology International*, Vol. 120, 2018, pp. 434-445, DOI: [10.1016/j.triboint.2018.01.023](https://doi.org/10.1016/j.triboint.2018.01.023)
- [12] SP Systems Guide to Composites, available at: https://composites.ugent.be/home_made_composites/documentation/SP_Composites_Guide.pdf, accessed: 30.01.2022.
- [13] H.F. Mark (Ed.), *Encyclopedia of Polymer Science and Technology*, John Wiley & Sons, Hoboken, 2002.
- [14] Hebatalrahman, Patent 24102: Four-Stroke Composite Material Machine, 2008.
- [15] H. Ahmed, Factors affecting irradiation of nano & micro materials by laser treatment industrial unit, *IOP Conference Series: Materials Science and Engineering*, Vol. 610, 2019, Paper 012005, DOI: [10.1088/1757-899X/610/1/012005](https://doi.org/10.1088/1757-899X/610/1/012005)
- [16] M. Banjac, A. Vencl, S. Otović, Friction and wear processes – Thermodynamic approach, *Tribology in Industry*, Vol. 36, No. 4, 2014, pp. 341-347.
- [17] M. Masjedi, M.M. Khonsari, A study on the effect of starvation in mixed elastohydrodynamic lubrication, *Tribology International*, Vol. 85, 2015, pp. 26-36, DOI: [10.1016/j.triboint.2014.12.014](https://doi.org/10.1016/j.triboint.2014.12.014)